Nanocomposites Prepared by Reactive Extrusion: Effect of the Polymer Reactive Groups

Manuel Oliveira, Ana Vera Machado*

The interest in the development of polymer nanocomposites by reactive extrusion has been growing in the past years. This work aims to investigate the effect of the polymer reactive groups on chemical reaction extension and consequently, on the morphology of the nanocomposites. For that, two polymers, polypropylene grafted with maleic anhydride (PP-g-MA) and ethylene vinyl acetate (EVA), are used as organic phases and aluminum isopropoxide ($Al(Pr-i-O)_3$) as metal. Nanocomposites are prepared in the melt using sol-gel process. The reaction extension is assessed by FT-IR, rheological measurements, and crosslinking density determination. The dispersion of inorganic nanoparticles is analyzed by SEM and TEM, and EDS is used to identify the presence of metal nanoparticles. Even though, both reactions are successfully accomplished in the melt, the reaction with EVA presents lower reaction activation energy (E_a) and the prepared nanocomposite has a more crosslinked structure. Moreover, a finer morphology with well-dispersed nanoparticles

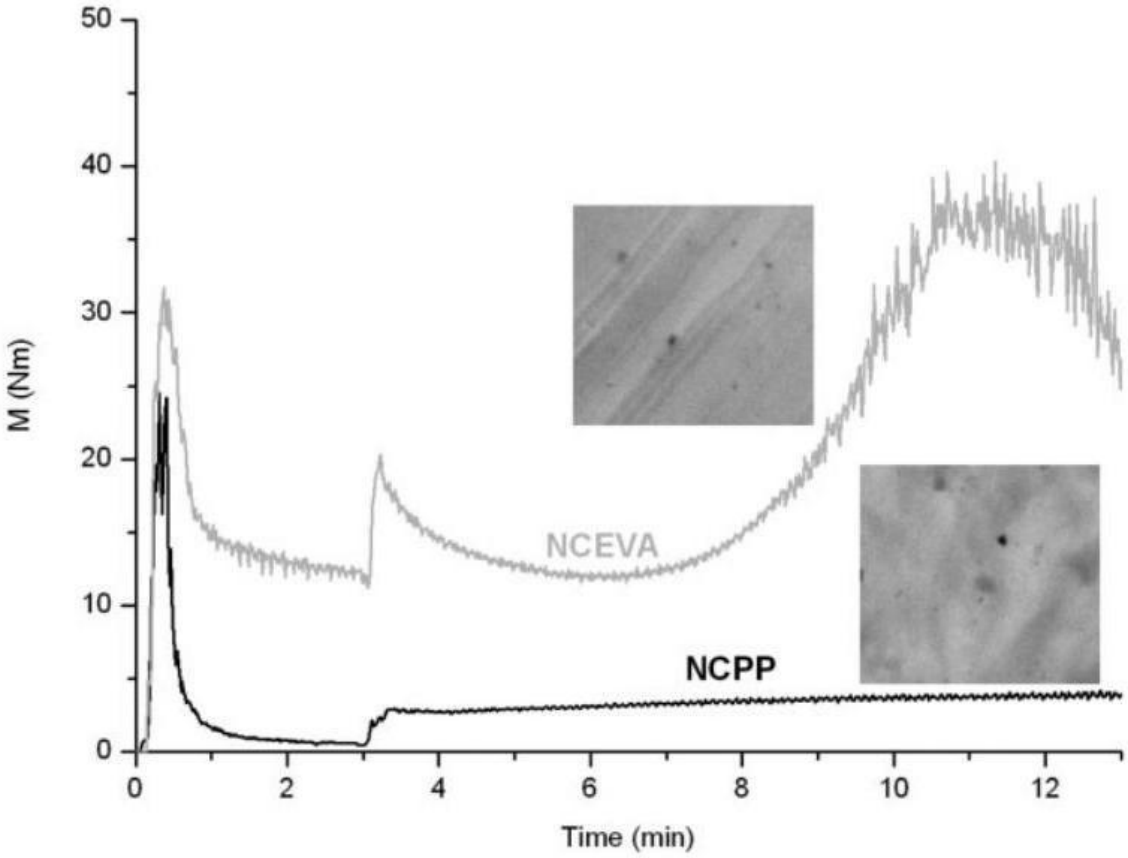

containing aluminum is achieved with EVA.

Introduction

Since ancient times, humans get used to mix organic and inorganic elements to obtain new materials with better properties. [1] Applying this principle to polymer science, it was found out that the dispersion of inorganic particles in a polymer matrix could improve significantly the polymer properties. [2] Polymeric nanocomposites appeared as a new class of materials, achieved by a well dispersion of a small amount of nano-size particles in a polymer matrix. These

materials can exhibit improved properties when compared to a conventional one, such as, gas permeability, thermal stability, flame retardance, electrical properties, mechanical performance, and chemical resistance. [3–5]

Even though a lot of researches have been performed on their preparation, [6–8] the best conditions to achieve homogeneous dispersion of nanoparticles in polymeric matrices, especially in apolar ones, still not defined. As the dispersion has a great effect on final nanocomposites properties, frequently these exhibit worst properties than conventional polymers, which limit their successful application. [9–11] In order to overcome the non-affinity issues between nanoparticles and polymer matrices, considerable attention has been devoted to improve synthesis processes and to develop new combined methods that could control the interfacial properties and consequently the dispersion quality.

Until now, three main approaches have been used to disperse nanoparticles in a polymeric matrix: solution dispersion, melting compounding and in situ nanoparticles formation by a sol-gel process. [12–14] Regarding to the dispersion of inorganic layered silicates or carbon nanotubes into a polymeric phase, it is often performed by melt compounding techniques that are readily available in industry, which provide good production yields and automatic operation, are environmentally friendly and capable to generate the hydrodynamic stresses required to achieve sufficiently good dispersion. Intermeshing corotating twin-screw extruders are particularly popular for this purpose. Nevertheless, this method has some drawbacks, it involves several parameters that are not easy to control, such as, interaction between the polymer matrix and the nanoparticles and processing conditions (temperature, stress, and residence time). [15] Therefore, in some cases can be difficult to obtain well-dispersed nanoparticles. The other approach that allows to overcome some of the negative points enumerated before is to perform sol-gel reactions in the melt. Some published studies demonstrated that this method, usually used in solution, can be suitable to produce dispersed nanoparticles in a polymer matrix, without solvent, with the advantage that can take place in an extruder and be used at industrial scale. [16–18] The process is based in a reaction between a metal alkoxide precursor, containing the inorganic particle and a molten polymer.

The interface between the nanoparticle and polymer plays a central role on the final nanocomposite properties. Based on it, two distinct categories are classified. While Class I has only weak bonds (hydrogen, van der Waals, or ionic), Class II has covalent bonds between organic and inorganic components. [19–22]

Bounor-Legaré et al. [18] described the synthesis EVA/ silica nanocomposites without presence of solvents. Using tetraalkoxysilane (TEOS) as silica nanoparticles precursor, EVA, and TEOS were mixed during 3 min at 110°C in an internal mixer in the presence of catalyst dibutyltin oxide. However, under these conditions only a physical mixing of the three compounds was obtained. The crosslinking reaction was then carried out at 150°C during 45 min between the plates of a hot press.

Dou et al. [13] investigated the preparation of PP/silica nanocomposite by direct sol-gel reaction in a twin-screw microcompounder. Aiming to perform the reaction in a single step, in opposite to other synthesis described in literature, they mixed hyperbranched PEOS with PP matrix in the presence of $Al(Pr-i-O)_3$ at 200°C for 18 min . Instead of obtaining a homogenous dispersion of particle with a diameter below 100 nm , the particle size was higher. This revealed poor interfacial interaction between organic and inorganic phases.

Bahloul et al. [14] reported a successful synthesis of a nanocomposite based on polypropylene containing titanium dioxide (PP/TiO_2) without presence of solvents.

Using a co-rotating twin-screw extruder, they prepared nacomposites of PP and titanium dioxide by injection of titanium *n*-butoxide at constant flow into the molten PP.

Even though, the sol-gel method has been investigated in the melt, there are many parameters that are not well understood and more studies are necessary in order to use this process to prepare materials with tailored properties. Therefore, the present work aims to assess the effect of the polymer reactive groups on the extension of sol-gel reaction and consequently on the nanocomposites morphology. Hence, two polymers with different

reactive groups (polypropylene grafted with maleic anhydride [PP-g-MA] and ethylene vinyl acetate [EVA] and a metal alkoxide [$Al(Pr-i-O)_3$]), with short organic chain and low chemical hindrance, was used as precursor to produce the inorganic nanoparticles. The reaction was performed in the melt and followed by FT-IR, crosslinking density, and rheological measurements. The activation energy (E_a) was also determined. Dispersion, average particle size and the presence of the metal in the polymer matrix were assessed by microscopic techniques, SEM, TEM, and EDS.

Experimental Section

Materials

Polypropylene modified with maleic anhydride (PP-g-MA, Polybond 3200) with a melting temperature around 160°C and a maleic anhydride content of 1wt%, was provided by Crompton. EVA with 27wt% of vinyl acetate (Escorene Ultra UL 00328, melting temperature of 71°C), was purchased by Exxon Mobil. Aluminum isopropoxide ($Al(Pr-i-O)_3$), used as received in powder state, was supplied by Sigma-Aldrich.

Processing

For both systems, the polymer and aluminum alkoxide concentrations were defined as 75/25w/w. The nanocomposites were produced by sol-gel process in melt mixing using a Haake batch mixer (Rheocord 90; volume 69 cm^3), equipped with two rotors running in a counter-rotating way. The rotor speed was 50 rpm and the set temperature was 100°C for EVA and 180°C for PP-g-MA nanocomposites, respectively. The materials were produced according to the following procedure, first pellets of the polymers were introduced into the hot mixer and after 3 min the aluminum precursor was added. The sol-gel reaction proceeded and after 10 min of mixing the total sample was removed. The nanocomposite (NC) synthesized with PP-g-MA was called NCPP, with EVA was NCEVA.

Materials Characterization

Oscillatory rheological measurements were carried out using a Paar Physica MCR300 rheometer at 180 and 100°C for NCPP and NCEVA, respectively. The gap and diameter of the plates was 1 and 25 mm , respectively. Nitrogen atmosphere was used to prevent thermooxidative degradation. A frequency sweep from 0.01 to 100 Hz under constant strain in the linear viscoelastic region was performed for each sample.

The crosslinking density of swollen polymers network are usually determine by Flory-Rehner model. The classical FloryRehner equation, directly relates the polymer volume fraction at swelling equilibrium to the average molecular weight between crosslinks, based on the elastic response of the polymer into the solvent. [23] A sample of 300 mg of polymer was immersed in hot xylene at 140°C during 30 h , the polymer volume fraction at swelling equilibrium, v_r, was determined using the follow equation:

$$v_r = \frac{1}{1 + (m_1/m_2)(\rho_2/\rho_1)} \quad (1)$$

where m_1 and m_2 are, respectively, the mass of solvent swelling the sample and the mass of dried crosslinking sample and ρ_1 and ρ_2 are, respectively, the polymer and solvent densities (gcm^{-3}).

The determination of the network density was based on the Flory-Rehner expression (Equation 2) coupled with the phantom network model gives a relation between the swelling results and the number of elastic strands, ν :

$$\nu = -\left[\frac{\ln(1-v_r) + v_r + \chi v_r^2}{V\left(v_r^{1/3} - 0.5v_r\right)}\right] \quad (2)$$

where χ is the polymer/solvent interaction parameter, V the molar volume of solvent and v_r is the polymer volume fraction at swelling equilibrium. Then, the polymer/solvent interaction parameter χ was calculated as followed:

$$\chi = \frac{V(\delta_1 - \delta_2)^2}{RT + 0.34} \quad (3)$$

where δ_1 and δ_2 are the solubility parameters of polymer and solvent, respectively, V is the molar volume; R is the universal gas constant; and T is the absolute temperature.

The activation energy (E_a) of the NCPP and NCEVA was estimated using gel content values. The nanocomposites were prepared at five different temperatures (170,175180,190, and 200°C for NCPP and 90,95,100,105, and 110°C for NCEVA, respectively) following the procedure described above and samples were collected after 3, 7, and 10 min of mixing. For all samples, the gel content was measured as described in Oliveira et al. [16] For each temperature, the crosslinking rate was determined as the slope of gel content versus time reaction, as described by Shieh et al. [24] Then, the E_a was calculated from the plot of the crosslinking reaction rate at the three different temperatures as a function of the reciprocal absolute temperature, according to the Arrhenius equation:

$$\ln k = \ln A - \frac{E_a}{R}\frac{1}{T} \quad (4)$$

where k is the crosslinking rate, E_a is the activation energy, R is the universal gas constant, and T is the absolute temperature.

Infrared spectra (FT-IR) measurements were recorded using a Jasco FTIR-4000 in transmission mode between 400 and 4000 cm^{-1}, with 64 scans and resolution of 4 cm^{-1}. Thin films were previously prepared by compression moulding in a hot press and analyzed directly using a solid film support.

Scanning electron microscopy (SEM) analysis was performed in a Leica Cambridge S360 microscope, samples were previously fractured in liquid nitrogen and coated with a gold thin film. The X-ray microanalysis mapping was performed on $300\mu^2$ in the same place where SEM micrographs were recorded, with an energy dispersive X-ray Spectrometer (EDS) from Link eXL II from Oxford Instruments attached to the microscope. Samples of 70 nm thickness for transmission electron microscopy (TEM) were cut using a diamond

knife, in a Leica ultramicrotome at -40 and −60°C for NCPP and NCEVA, respectively. The cut sections were transferred onto copper grids and then analyzed without staining in a Philips CM120 microscope.

Results and Discussion

When an internal mixer is used as a chemical reactor the torque evolution along the mixing time gives important information about the synthesis success. Figure 1 shows the torque evolution during the preparation of NCPP and NCEVA, respectively. The first peak is associated to polymer melting followed by the addition of the aluminum precursor. The effect of the addition of aluminum precursor on PP and EVA matrices is clear, the torque increased for both polymers, but it was more accentuated for EVA. The torque behavior is due to the crosslinking reaction between maleic anhydride or vinyl acetate groups, respectively, with aluminum precursor. From the torque evolution, it can be anticipated that NCEVA has a more crosslinked structure, which can be associated to two factors, the stereochemical hindrance of the reactive group and the amount of vinyl acetate and maleic anhydride groups that were 27 and 1 wt% for EVA and PP, respectively. Another important

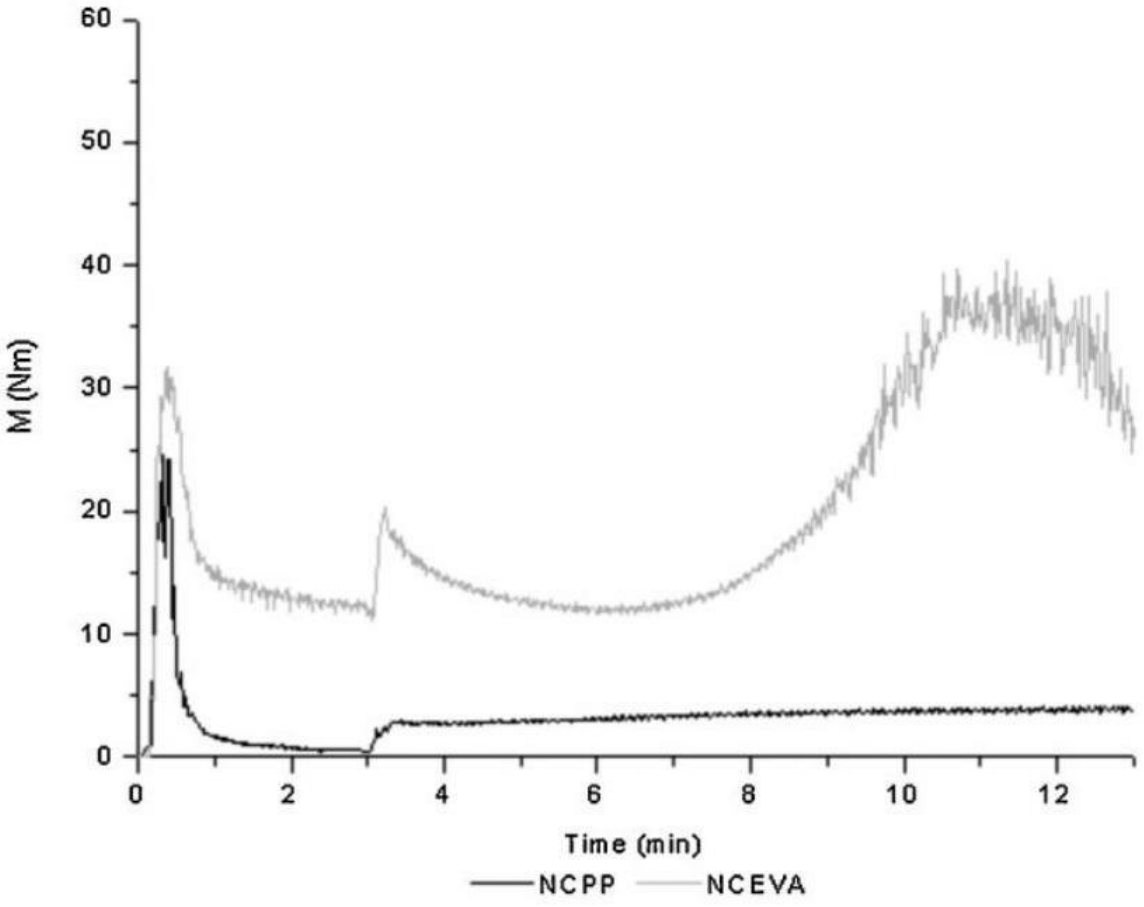

Figure 1. Torque evolution along time during NCPP and NCEVA preparation. feature is that the torque decreases after 11 min of mixing. This is a typical phenomenon for materials with very high crosslinking contents, and can be attributed to the network

degradation as shown by Antunes et al. [25] Contrarily, for PP the torque increased instantaneously when $Al(Pr-i-0)_3$ was added, but after was almost constant.

The rheological behavior of original polymers and the respective nanocomposites is depicted in Figure 2. A strong increase in storage modulus and complex viscosity can be detected. The materials behavior changes from liquid-like to solid-like, where the storage modulus is independent of the frequency value. The nanocomposites prepared do not show a plateau at low frequencies and the complex viscosity has, in the limit, a slope of minus one. [26] Based on the curves, slope values of -0.957 and -0.885 for NCPP and NCEVA, respectively, were obtained. The observed increase in viscosity and storage modulus for both nancomposites could be associated to three causes: first due to the presence of inorganic filler dispersed in the polymeric matrices, second due to physical interaction, and third by the formation of a branched/crosslinking structures. Then, for further confirmation, gel content and the crosslinking density (Table 1) were determine for each nanocomposite.

The gel content and crosslinking density values, presented in Table 1, confirm the presence of a crosslinking network on both nanocomposites. Solubility measurements using xylene as solvent showed that the weight ratio of the crosslinked structure of the final nanocomposites was around 70%. The gel content and crosslinking densities are slightly higher for EVA, which would be anticipated from the torque behavior.

The processes activation energies (E_a) were determined to better understand the previous results. Using the Arrhenius

Table 1. Gel content values and crosslinking density obtained for NCPP and NCEVA after synthesis reactions.

Samples	Gel content [%]	Crosslinking density [mol mL^{-1}]
NCPP	69.2 ± 3.4	$(10.5 \pm 0.2) \times 10^{-5}$
NCEVA	73.2 ± 0.3	$(11.3 \pm 0.8) \times 10^{-5}$

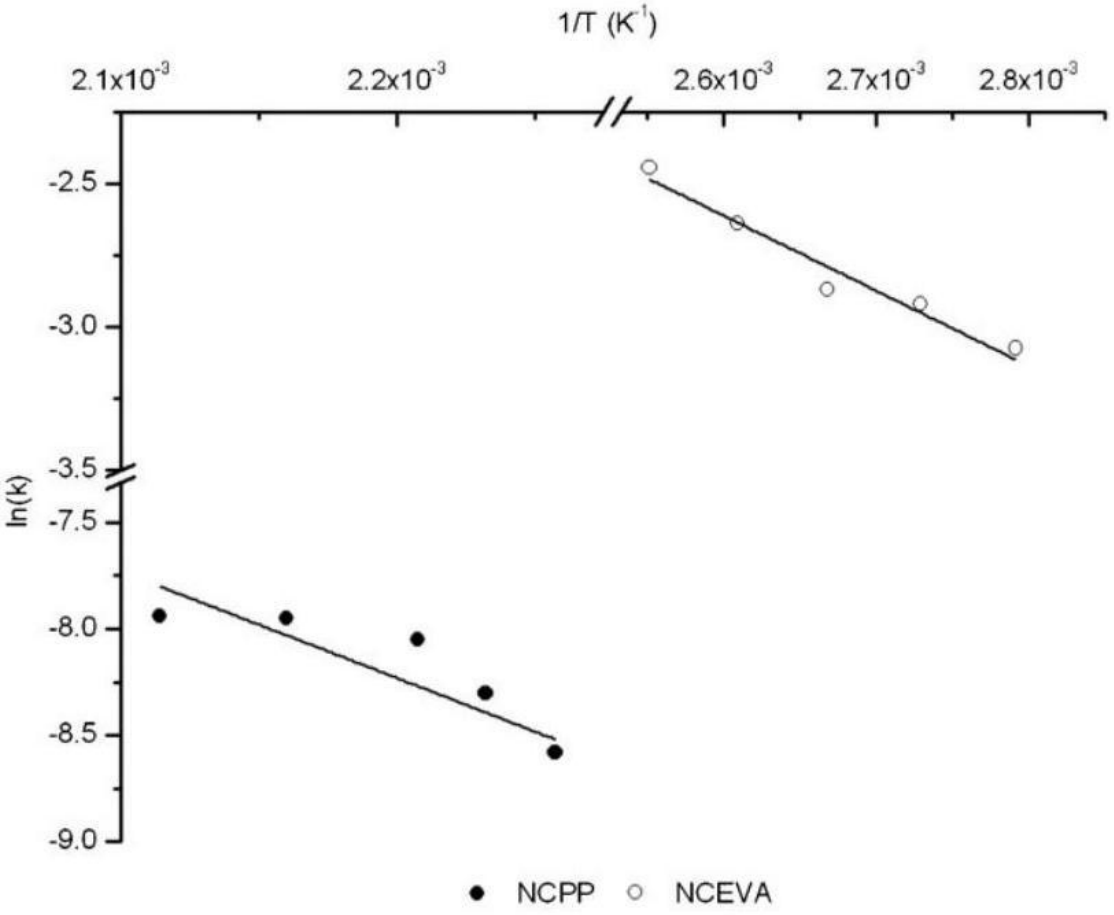

Figure 3. Arrhenius plots for the synthesis reactions of NCPP and NCEVA. equation (Figure 3) a linear relationship was found for both nanocomposites, corresponding to an E_a of 52.9 and 36.3 kJ mol^{-1} for NCPP and NCEVA, respectively. The lower E_a required for EVA can be explained by the

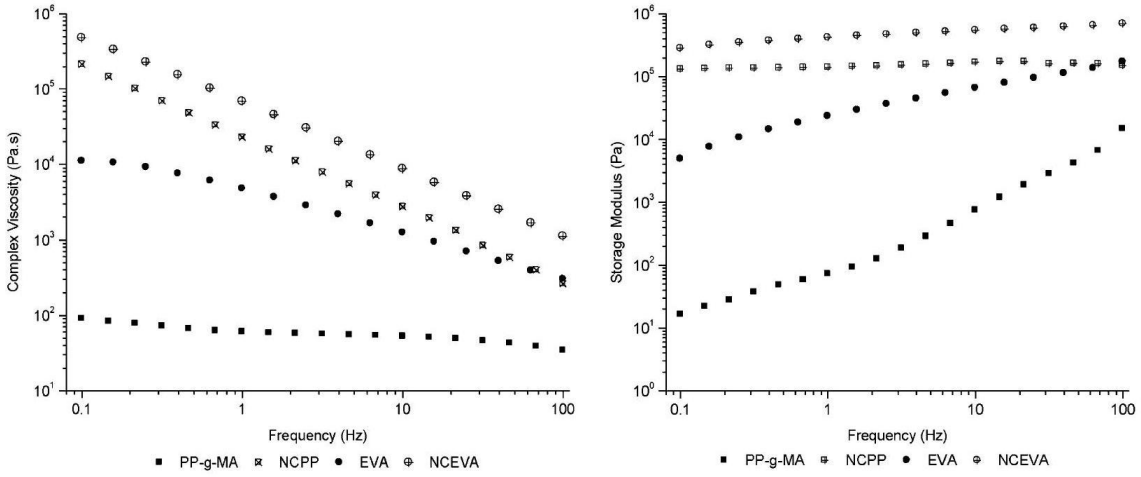

□ Figure 2. Rheological behavior of PP-g-MA, EVA, NCPP, and NCEVA. higher amount of vinyl acetate groups and their lower stereochemical hindrance when compared with maleic anhydride groups grafted on PP. Therefore, this data are in agreement with the higher crosslinking density of NCEVA.

FT-IR analysis were performed to acquired information on the chemical struture of the prepared nanocomposites and also on the reaction mechanism. A comparison of the PP-g-MA and NCPP spectra (Figure 4a) indicates that before reaction the anhydride groups is mainly in the acid form, the absorsorption band at 1733 cm^{-1} correspondent to the hydrolysed product is much intense than the one at 1785 cm^{-1} associated with the close form. After reaction a strong reduction of the bands intensity at 1785 and 1733 cm^{-1} can be detected, which indicates that almost all groups reacted.

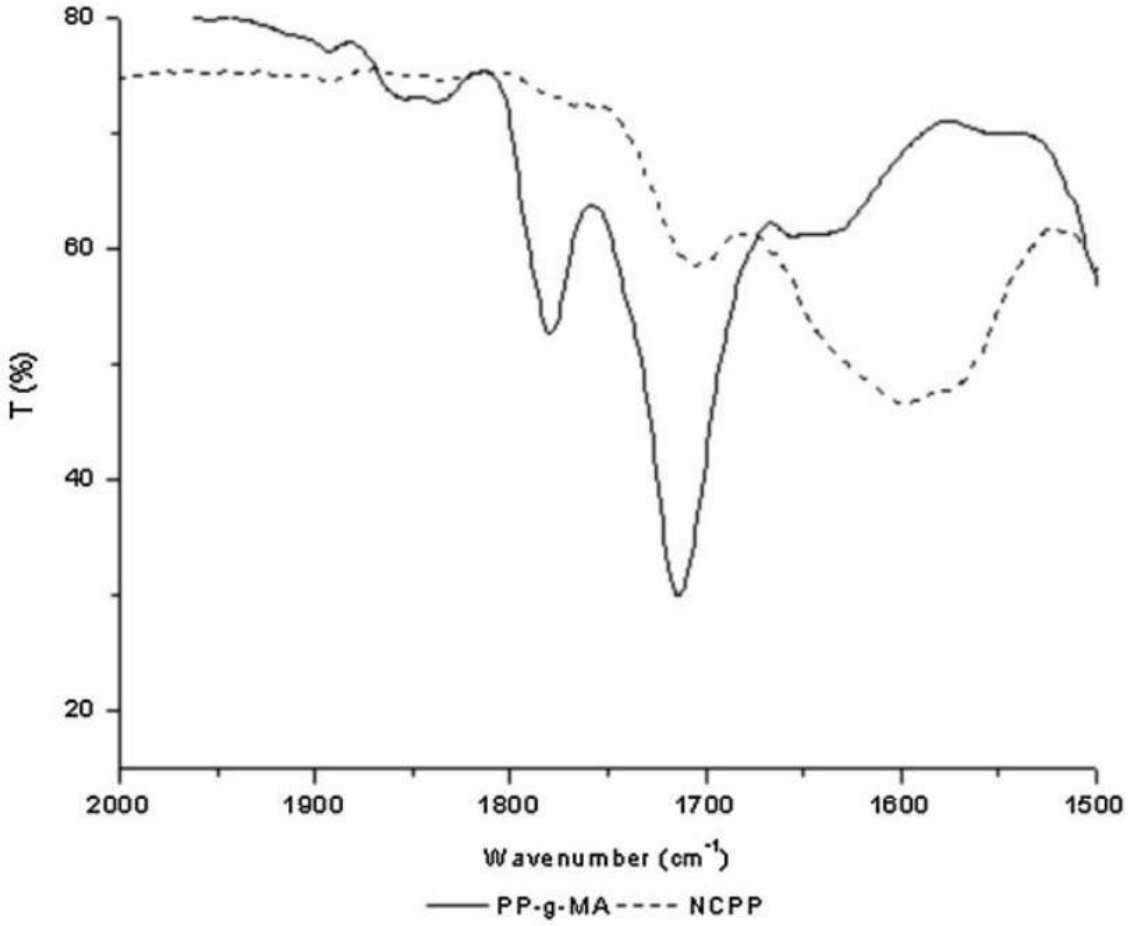
80
60
40
20
T (%)
2000
1900
1800
1700
1600
1500
Wavenumber (cm-1)
PP-g-MA
NCPP

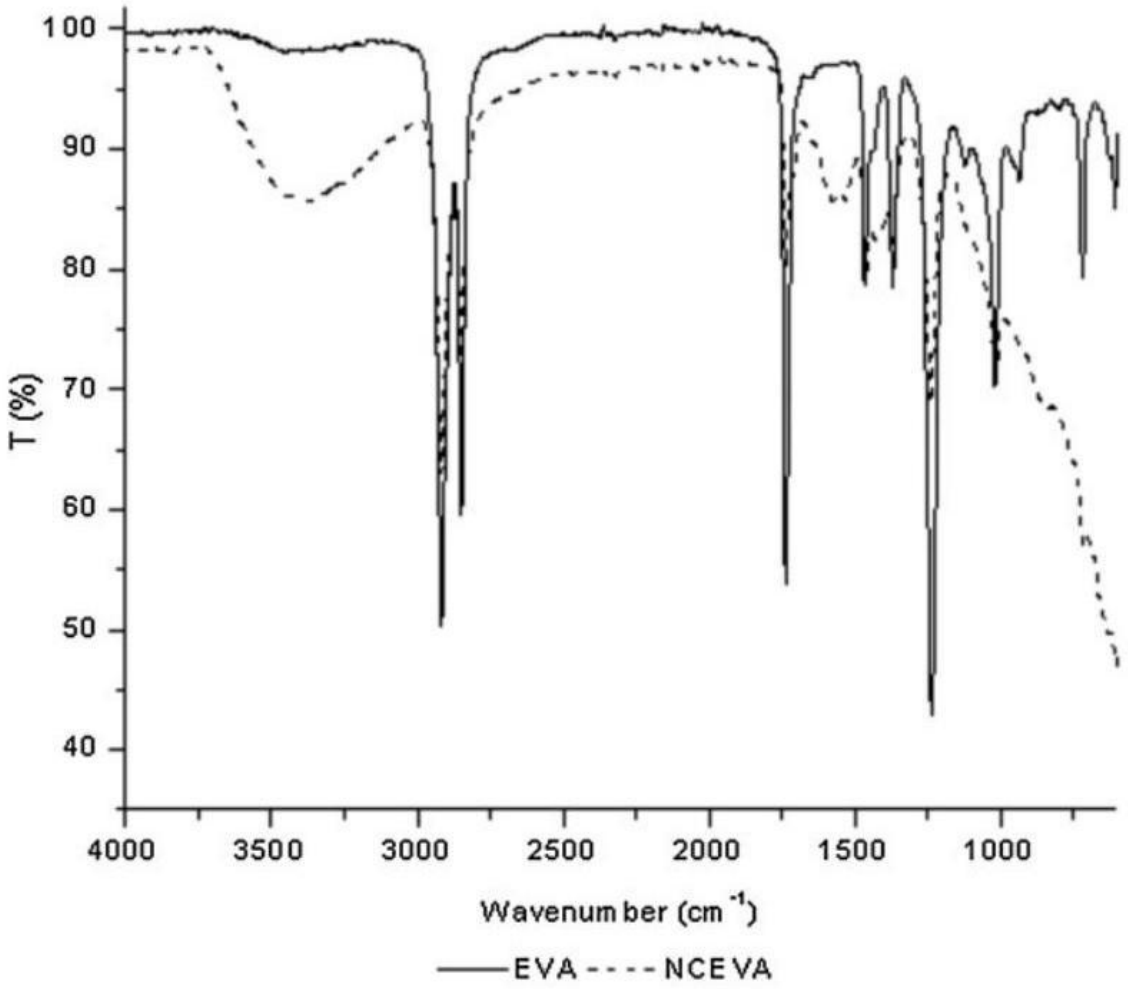

Figure 4. FT-IR of a) maleic anhydride of PP-g-MA and NCPP; b) FTIR-ATR of EVA and NCEVA.

In the case of NCEVA (Figure 4b), differences can also be noticed in the peak of the $C = O$ stretching mode of the acetate group. After reaction, the intensity of the band becomes lower that clearly reveals a reduction on the amount of acetate groups.

Moreover, as depicted in Figure 5, NCPP and NCEVA show new absorption bands when compared with the initial polymers. A comparison of these spectra evidences, for both nanocomposites, a very broad band around $3450\ cm^{-1}$, which corresponds to the streching mode of $Al - OH$ and carboxilic acid of maleic acid being confirmed by the respective bending mode at $1627\ cm^{-1}$. The aluminum can be bonding to polymeric matrix by two different coordination states, octahedral or tetrahedral. [27,28] Octahedral coordintaion is defined by stretching mode band in the region of $640 - 500\ cm^{-1}$, while tetrahedral coordination by stretching mode band between 500 and $750\ cm^{-1}$. Then, tetrahedral coordination seems to prevail for both nanocomposites.

Then, based on the results discussed above, the schemes of Figure 6 represent a simplified reaction mechanism involved in the preparation of the two nanocomposites.

The dispersion and the nanoparticles size were assessed by SEM and TEM analysis (Figures 7 and 9). SEM images show that NCEVA have a smoother surface when compared to NCPP, however in both cases the presence of inorganic agglomerates cannot be detected, which can be an indication of homogenous dispersion. The presence of aluminum species at the surface analyzed by SEM was confirmed by EDS (Figure 8). Aluminum contents of 4% and 5% were determined to NCPP and NCEVA, respectively. This amount is lower than the theoretical (7%), which can be explained by the lost of some precursor during feeding or different homogeneity of the samples. TEM micrographs

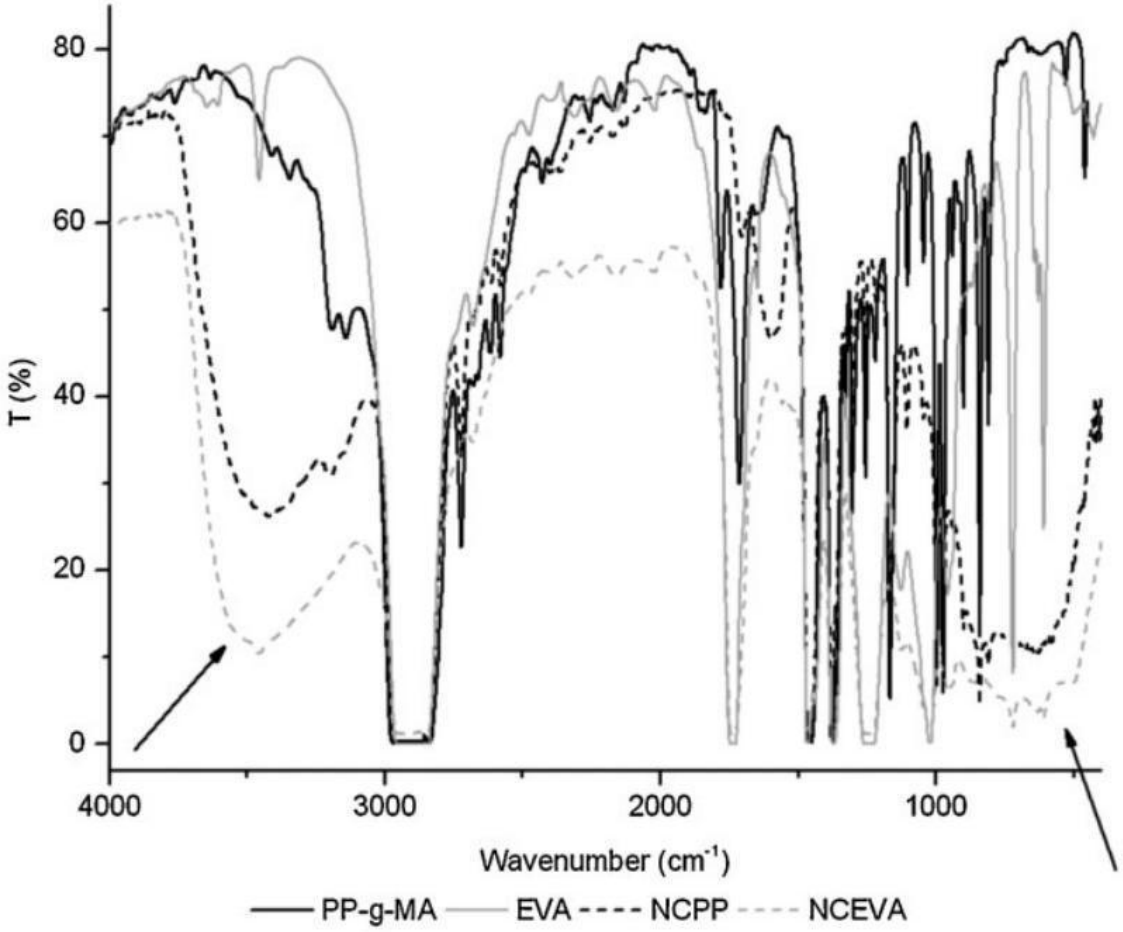

Figure 5. FT-IR spectra of PP-g-MA, EVA, NCPP, and NCEVA.

OH OC OH

b)

CH3.

Figure 6. Reaction mechanism of a) NCPP and b) NCEVA.

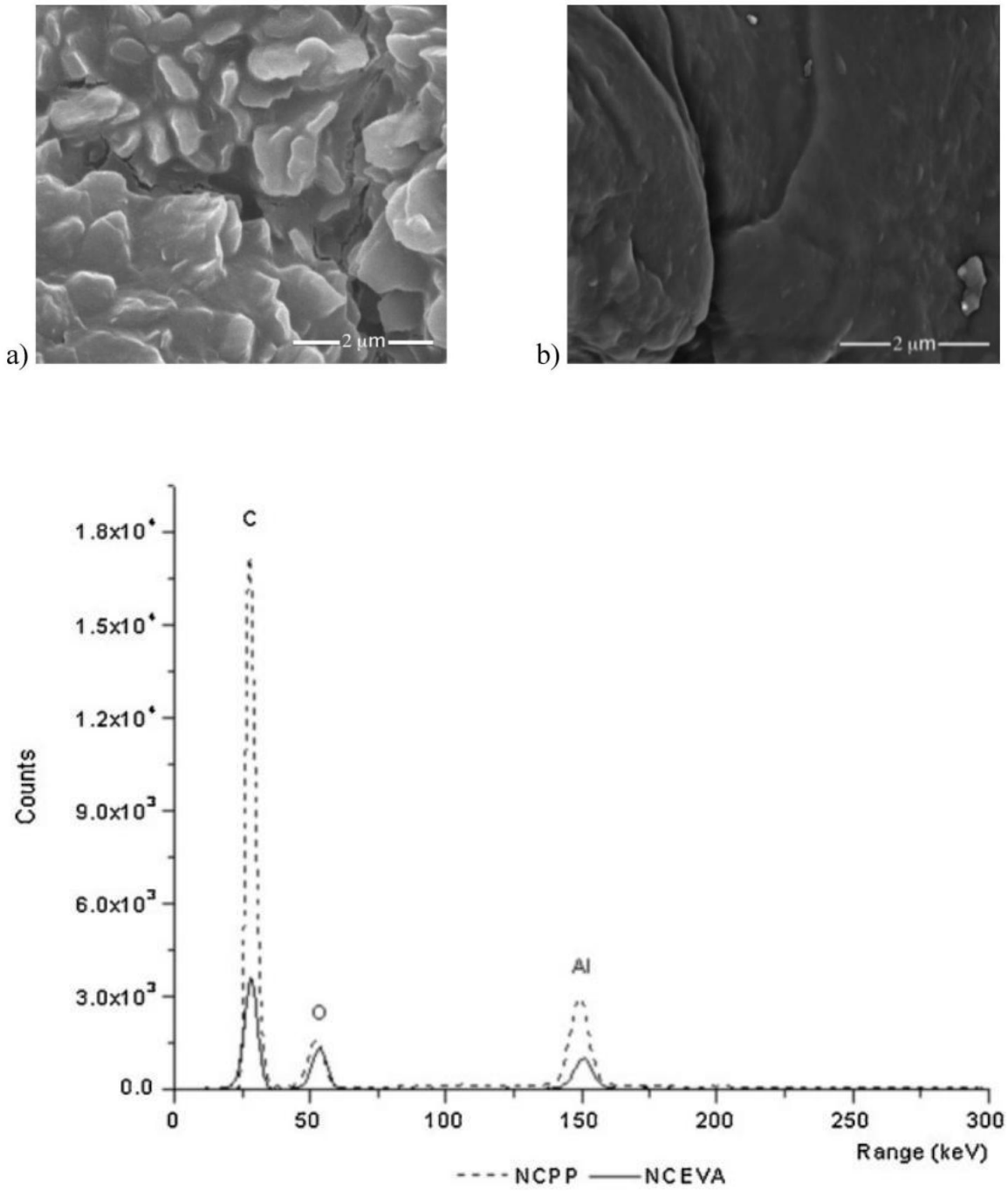

Figure 8. EDS spectra of NCPP and NCEVA.

confirm that a fine dispersion of nanoparticles containing aluminum was achieved (Figure 9). Nevertheless in EVA matrix the particles are smaller (120 nm) than in PP (200 nm). Moreover, the number of particles per area was also higher for EVA ($2.1/\mu m^2$) than for PP ($1.7/\mu m^2$). Better dispersion and smaller particles can be associated with higher reactivity between the precursor and the vinyl acetate groups.

Conclusion

In this work, the effect of the polymer reactive groups was investigated on the preparation of organic inorganic nanocomposites by in situ sol-gel process in the melt. New materials with nanoparticles containing aluminum
a)

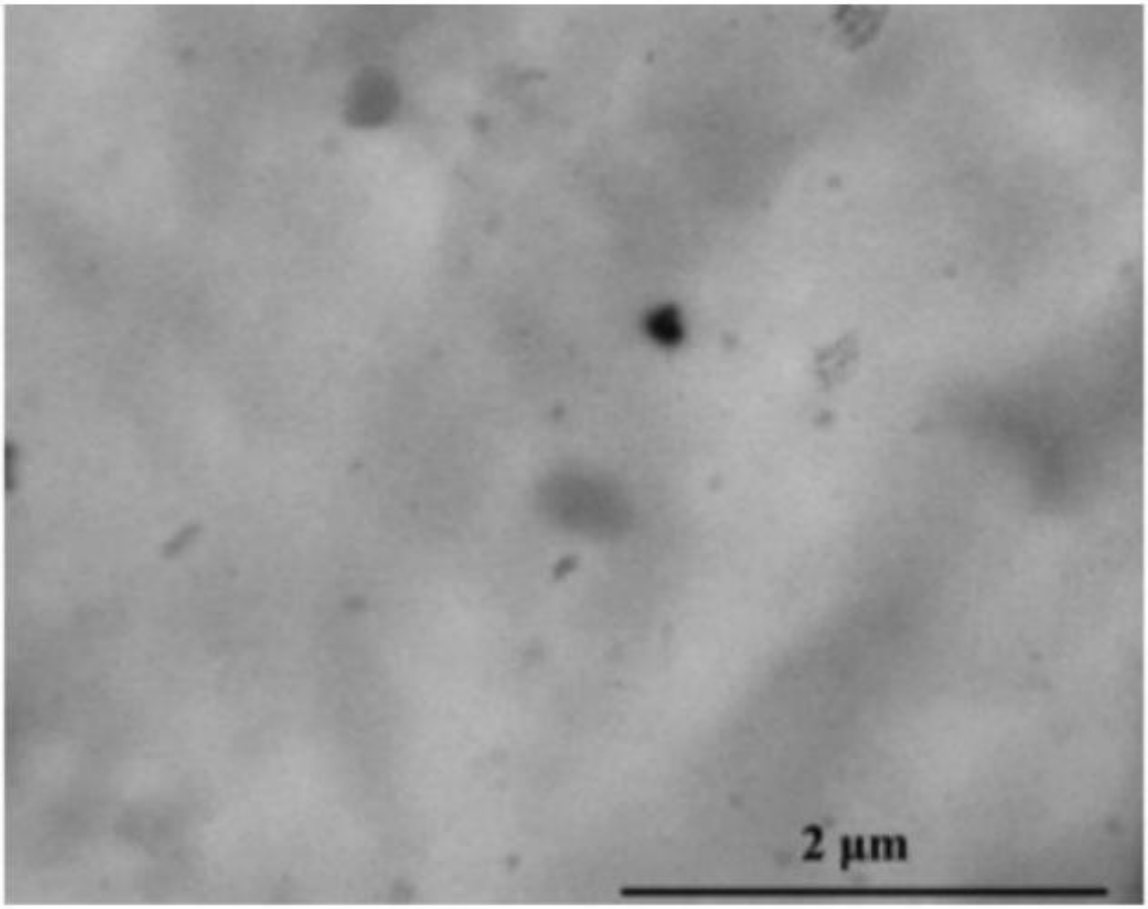

Figure 9. TEM micrographs of a) NCPP and b) NCEVA.
bonded by covalent bonds to polymers chains were obtained, resulting in change from a liquid-like behavior to a solid-like behavior with a storage modulus independent of the frequency. Even though, both reactions were successfully accomplished in the melt, the reaction with EVA presents lower reaction activation energy (E_a) and the prepared nanocomposite has a more crosslinked structure. Moreover a finer morphology with welldispersed nanoparticles containing aluminum was achieved with EVA. Therefore, the nature of the chemical groups presented or grafted in polymeric backbone play an important role on reactivity and consequently on properties.

The present study demonstrates that is possible to prepare nanocomposites with different properties by changing the polymer reactive groups. Furthermore, it is feasible to apply the sol-gel process in the melt without use of solvents, turning it suitable for industrial application.

Acknowledgments: The authors acknowledge the Foundation for Science and Technology (FCT) Project SFRH/BD/39085/2007 and PEst-C/CTM/LA0025/2011 for the financial support.

Received: May 17, 2013; Revised: July 9, 2013; Published online: September 16, 2013; DOI: 10.1002/mren. 201300132

Keywords: polymer nanocomposites; reactive extrusion; sol-gel reactions
[1] C. Sanchez, B. Julián, P. Belleville, M. Popall, J. Mater. Chem. 2005, 15, 3559.
[2] R. Krishnamoorti, R. A. Vaia, Polymer nanocomposites Synthesis, characterization & modeling, ACS symposium series 2002.
[3] W. Bahloul, V. Bounor-Legaré, L. David, P. Cassagnau, J. Polym. Sci., Part B: Polym. Phys. 2010, 48, 1213.
b)

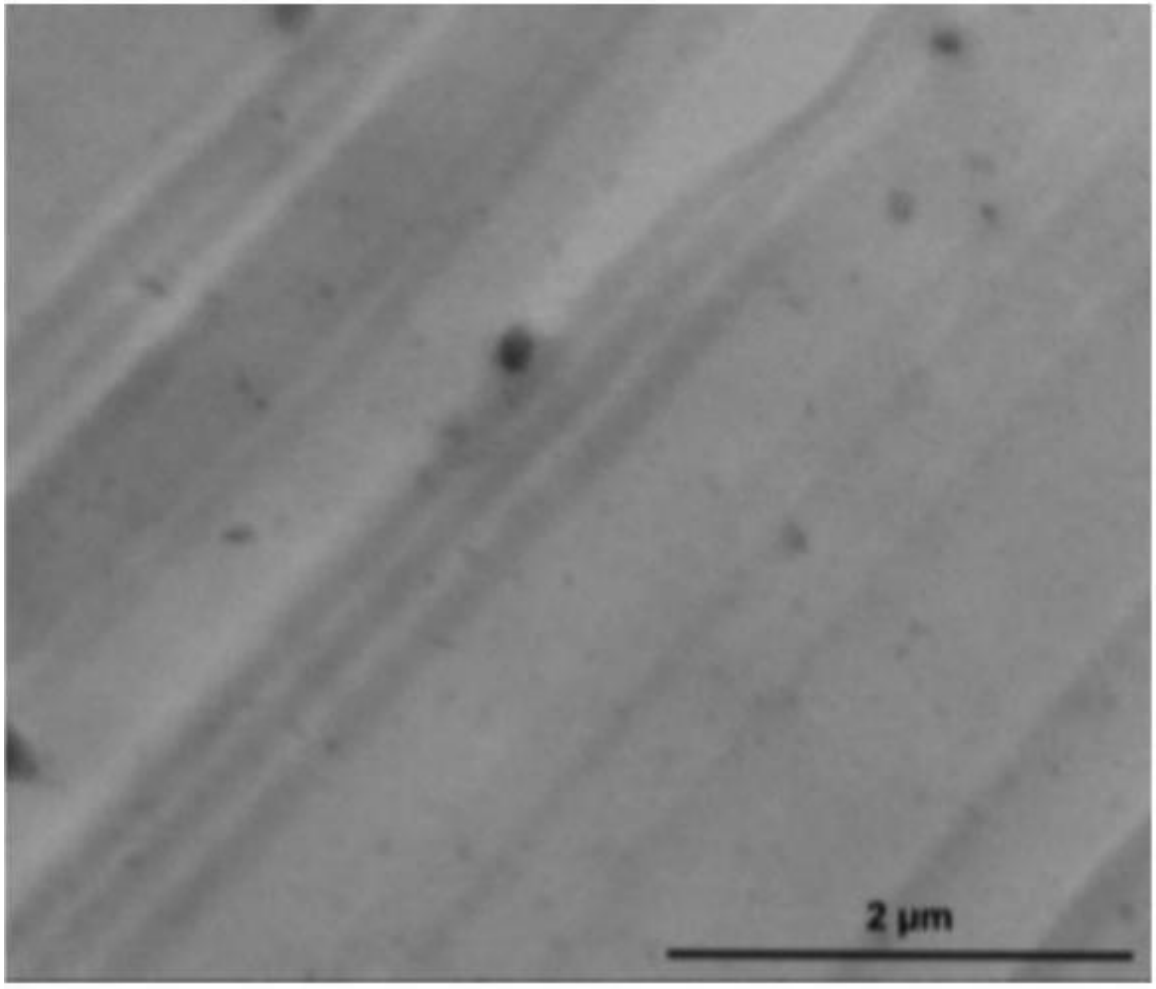

[4] M. Sadeghi, G. Khanbabaei, A. H. S. Dehaghani, M. Sadeghi, M. A. Aravand, M. Akbarzade, S. Khatti, J. Membr. Sci. 2008, 322, 423.
[5] C. Sanchez, K. Shea, S. Kitagawa, Chem. Soc. Rev. 2011, 40, 453.
[6] P. Judeinstein, C. Sanchez, J. Mater. Chem. 1996, 6, 511.
[7] US. 3891594, inv. L. J. Taylor; US Patent, 1975.
[8] K. H. Wang, M. H. Choi, C. M. Koo, Y. S. Choi, I. J. Chung, Polymer 2001, 42, 9819.
[9] X. Liu, Q. Wu, Polymer 2001, 42, 10013.
[10] M. Z. Rong, M. Q. Zhang, Y. X. Zheng, H. M. Zeng, K. Friedrich, Polymer 2001, 42,

3301.
[11] C. Xu, K. Ohno, V. Ladmiral, R. J. Composto, Polymer 2008, 49, 3568.
[12] Y. Di, S. Iannace, E. Di Maio, L. Nicolais, J. Polym. Sci., Part B: Polym. Phys. 2003, 41, 670.
[13] Q. Dou, X. Zhu, K. Peter, D. Demco, M. Möller, C. Melian, J. SolGel Sci. Technol. 2008, 48, 51.
[14] W. Bahloul, O. Oddes, V. Bounor-Legaré, F. Mélis, P. Cassagnau, B. Vergnes, AlChE J. 2011, 57, 2174.
[15] H. Fischer, Mat. Sci. Eng.: C 2003, 23, 763.
[16] M. Oliveira, R. Nogueira, A. V. Machado, React. Funct. Polym. 2012, 72, 703.
[17] M. Oliveira, R. Nogueira, A. V. Machado, Adv. Polym. Tech. 2012, 32 S1, E732.
[18] V. Bounor-Legaré, C. Angelloz, P. Blanc, P. Cassagnau, A. Michel, Polymer 2004, 45, 1485.
[19] F. Hussain, M. Hojjati, M. Okamoto, R. E. Gorga, J. Compos. Mater. 2006, 40, 1511.
[20] C. Sanchez, P. Belleville, M. Popall, L. Nicole, Chem. Soc. Rev. 2011, 40, 696.
[21] G. Z. Cao, Y. Wang, Nanostructures and Nanomaterials: Synthesis, Properties, and Applications, 2nd ed., Imperial College Press, London 2011.
[22] S. Yano, K. Iwata, K. Kurita, Mater. Sci. Eng: C 1998, 6, 75.
[23] A. Vieyres, R. Pérez-Aparicio, P.-A. Albouy, O. Sanseau, K. Saalwächter, D. R. Long, P. Sotta, Macromolecules 2013, 46, 889.
[24] Y.-T. Shieh, J.-S. Liau, T.-K. Chen, J. Appl. Polym. Sci. 2001, 81, 186.
[25] C. F. Antunes, A. V. Machado, M. van Duin, Rubber Chem. Technol. 2009, 82, 492.
[26] V. Bounor-Legaré, I. Ferreira, A. Verbois, P. Cassagnau, A. Michel, Polymer 2002, 43, 6085.
[27] I. H. Joe, A. K. Vasudevan, G. Aruldhas, A. D. Damodaran, K. G. K. Warrier, J. Solid State Chem. 1997, 131, 181.
[28] J. H. Wengrovius, M. F. Garbauskas, E. A. Williams, R. C. Goint, P. E. Donahue, J. F. Smith, J. Am. Chem. Soc. 1986, 108, 982.